LA-UR-10-04266

Approved for public release;
distribution is unlimited.

Title: MCNP/X Form Factor Upgrade for Improved Photon Transport

Author(s): J.S. Hendricks & B.J. Quiter

Intended for: Nuclear Technology, Vol. 175, July 2011

MCNP/X FORM FACTOR UPGRADE FOR IMPROVED PHOTON TRANSPORT

PHOTON TRANSPORT AND SHIELDING (DETERMINISTIC OR MC)

KEYWORDS: *Monte Carlo, photoatomic, form factor*

JOHN S. HENDRICKS[a,b,c]* and BRIAN J. QUITER[d,e]

[a]*TechSource, Inc., Los Alamos, New Mexico 87544*
[b]*Los Alamos National Laboratory, Los Alamos, New Mexico 87545*
[c]*Brookhaven National Laboratory, Upton, New York 11973*
[d]*University of California, Department of Nuclear Engineering Berkeley, California 94720*
[e]*Lawrence Berkeley National Laboratory, Berkeley, California 94720*

Received February 9, 2010
Accepted for Publication June 28, 2010

The angular distribution of scattered photons is incorrect in MCNPX and MCNP5 because the incoherent and coherent form factors are obsolete. The obsolete data affect all photon transport problems with $E > 74$ keV. Elastic backscatter for $E > 105$ keV is completely missing. Consequently, a new ACE-format photoatomic data library, tentatively named MCPLIB05 and referred to herein as MCPLIB05T, has been developed for MCNP/X. Data in MCPLIB05T other than form factors are identical to that in its predecessor photoatomic library, MCPLIB04. The new form factor data in MCPLIB05T come directly from ENDF/B-VII (rev. 0) and are in a format incompatible with older versions of MCNP/X. Consequently, a new version of MCNP/X has been developed to identify and use the new MCPLIB05T data and yet retain backward compatibility, including tracking, when MCPLIB04 is used. The NJOY nuclear data processing system is undergoing development to enable future generations of photoatomic data libraries with modern form factor data in the new format.

I. INTRODUCTION

I.A. Motivation

The coherent scattering form factor and the related incoherent scattering function are multiplicative corrections to the Thomson and Klein-Nishina scattering cross sections, respectively, that modify photon scattering cross sections to account for the effects of atomic electron binding. These corrections are both considered to be form factors. The inadequacies of the MCNP/X (Refs. 1 and 2) form factors were identified by simulating the scattered photon background encountered in nuclear resonance fluorescence (NRF) experiments.[3] These inadequacies were also independently observed by Lodwick and Spitz[4] in an in vivo X-ray fluorescence measurement of stable lead in bone.

Simulations attempting to reproduce data obtained in NRF experiments found that simulations using MCNPX of a 2-MeV endpoint energy bremsstrahlung photon beam striking a uranium target underestimated the 135-deg backward scattered photon background by a factor of ~4 at 1.7 MeV and up to several orders of magnitude near 2 MeV. This error was because the elastic scatter coherent form factors were too coarsely defined in the predecessor code MCP (Ref. 5), written in 1973, and while the coherent scatter form factor array has been updated numerous times since then, the form factor array in MCNP/X remained unchanged. These data were specified on a fixed grid of 21 points for incoherent form factors (also referred to as the incoherent scattering function) applied to Compton scattering and 55 points for coherent form factors applied to Thomson scattering. The grid is in units of inverse angstroms and for coherent scatter the maximum value allowed in MCNP/X was 6 $Å^{-1}$ even though the evaluated photon data library[6] (EPDL'97), which is the basis of ENDF/B-VII photoatomic data,[7] allows values up to 1×10^{11} $Å^{-1}$. Consequently, the truncated form factors make all the 1.7-MeV photons undergoing coherent Thomson scattering on uranium go within 5 deg of

*E-mail: jxh@lanl.gov

the forward direction, completely eliminating elastic backscatter for angles >5 deg of the forward direction.

I.B. Effect on Transport Problems

Fortunately, the large errors in photon elastic scattering angular distributions generally have a negligible effect on most transport problems. The effect of the incorrect angular distributions is greatest at high energies where the Thomson scattering cross section is small relative to the competing channels of incoherent (Compton) inelastic scatter, photoelectric fluorescence, and pair production. Also, the truncated form factor effect is greatest for high-Z materials where incoherent scatter and pair production are even more significant.

The effect of truncated form factors is significant only when looking at the photon energy spectrum resulting from backscattering of energetic photons. Compton scatter, photoelectric fluorescence, and pair production all emit photons of lower energy than the incident energy, and the elastic Thomson scatter photons stand out with their unchanged energy. For these coherent scatters the truncation of the form factors is most pronounced.

I.C. Photon Reactions

Photon physics in MCNP/X is simple relative to neutron physics. There are only five possible scattering mechanisms and there are no angular distribution tables. These mechanisms are:

1. *incoherent scatter*: Klein-Nishina + *form factors*; Doppler broadening (electron binding) optional
2. *coherent scatter*: Thomson + *form factors*
3. *photoelectric*: absorption + 1st, 2nd fluorescence
4. *pair production*: + annihilation photons (0.511 MeV)
5. *bremsstrahlung*: electron production emitting bremsstrahlung photons (optional).

The process by which photons are effectively scattered by bremsstrahlung is complex and requires generation of photon-induced electrons to subsequently produce bremsstrahlung progeny. Pair production results in two annihilation photons of 0.511 MeV in opposite directions from an isotropically chosen direction. Photoelectric fluorescence requires secondary photon energy distribution data, but the angular distributions are all isotropic. The secondary energy and angle distributions of incoherent and coherent scatter are determined from the Klein-Nishina and Thomson formulas, respectively, rather than data tables as is the case for the more complicated neutron transport.

Photon interaction cross sections all look qualitatively similar to the W ($Z = 74$, tungsten) photon cross sections plotted in Fig. 1.

TABLE I

Percentage of the Incoherent and Coherent Cross Sections Relative to the Total Cross Section for a Number of Different Elements at $E = 105$ keV, the Energy at Which MCPLIB04 Form Factors Disallow Any Backward Scatter ($\mu < 0$)

Z	Incoherent	Coherent
1	33.0%	0.03%
9	76.5%	3.57%
24	42.5%	9.97%
45	10.1%	6.85%
88	1.7%	2.84%
92	5.7%	11.3%

The incoherent and coherent cross sections are generally dwarfed by the photoelectric and pair production cross sections, both of which have isotropic angular scattering distributions. Thus, the forward-peaked coherent scatter is often insignificant, as seen in Table I.

I.D. Incoherent Cross Sections and Form Factors

The photoatomic incoherent cross section is

$$\sigma_I(Z,\alpha,\mu)\,d\mu = I(Z,\nu)K(\alpha,\mu)\,d\mu \ , \qquad (1)$$

where

$$K(\alpha,\mu)\,d\mu = \pi r_o^2(\alpha'/\alpha)^2[\alpha'/\alpha + \alpha/\alpha' + \mu^2 - 1]\,d\mu \qquad (2)$$

is the Klein-Nishina cross section and where

r_o = classical electron radius, 2.817938×10^{-13} cm

μ = cosine of the polar scattering angle (azimuthal symmetry assumed)

α, α' = incident and final photon energies, respectively, in units of 0.511 MeV ($\alpha = E/mc^2$, where m is the mass of the electron and c is the speed of light)

$\alpha' = \alpha/[1 + \alpha(1 - \mu)]$.

The incoherent form factor $I(Z,\nu)$ is a function of Z and the momentum, where ν is the inverse length in angstroms, Å^{-1}. Its values are illustrated in Fig. 2.

In MCPLIB04 (Ref. 8) the incoherent form factor $I(Z,\nu)$ is truncated at momentum transfer $\nu = 8\ \text{Å}^{-1}$; that is, $E > 0.1402687/\sqrt{1-\mu}$ MeV. Above this momentum, MCNP/X sets the form factor to 1, resulting in the small (<6%) errors to the incoherent form factor listed in Table II.

Qualitatively, the effect of $I(Z,\nu)$ is to decrease the Klein-Nishina cross section (per electron) more extremely in the forward direction, for low E and for high Z independently. Because the scattering angle and energy

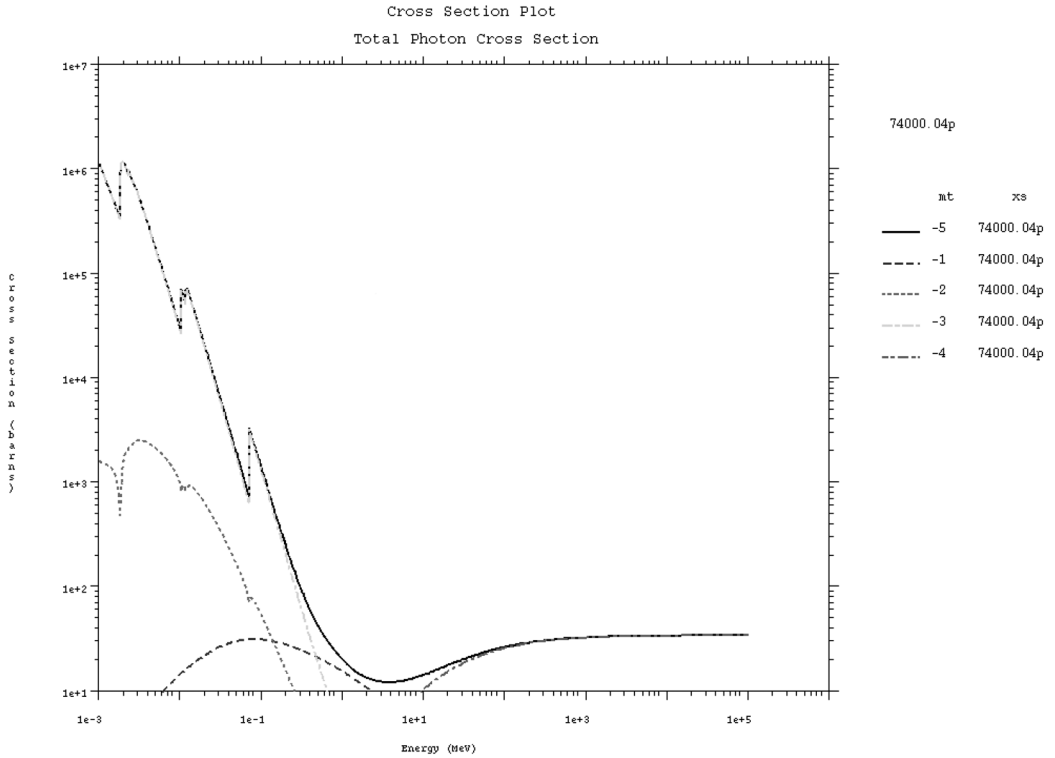

Fig. 1. MCNPX plot of W ($Z = 74$, tungsten) photoatomic cross sections versus energy, $10^{-3} < E < 10^{-5}$ MeV. Black (solid line, highest overall) = total; blue (dashed line, hump on left) = incoherent; red (dashed line, middle on left) = coherent; green (broken line, highest on left) = photoelectric; and purple (broken line, rising on right) = pair production (color online). The coherent reactions are usually dwarfed by the isotropically scattering photoelectric and pair production reactions.

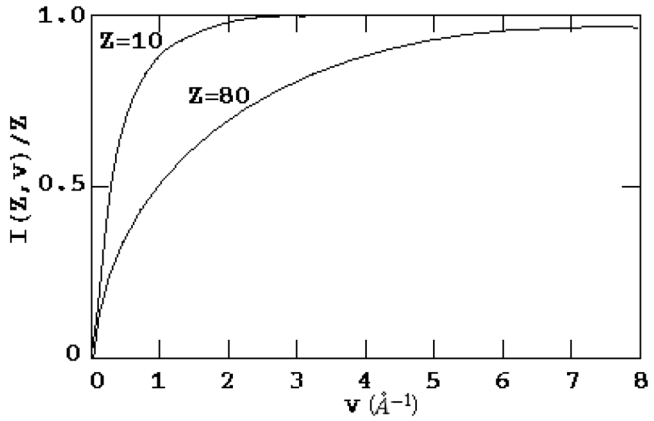

Fig. 2. Incoherent photoatomic scattering form factors.

TABLE II

Errors in Incoherent Form Factors for $\nu > 8$

Z	$1.0 - I(Z,\nu)$
12	0.00017
32	0.0104
60	0.0293
92	0.0498
98	0.0597
100	0.0554

are directly linked by the Klein-Nishina formula, this results in a lower energy spectrum.

I.E. Coherent Cross Sections and Form Factors

The photoatomic coherent cross section is

$$\sigma_C(Z,\alpha,\mu)\,d\mu = C^2(Z,\nu)T(\mu)\,d\mu \ , \qquad (3)$$

where

$$T(\mu)\,d\mu = \pi r_o^2(1+\mu^2)\,d\mu \ . \qquad (4)$$

Here, $T(\mu)$ is the Thomson cross section. The coherent form factor $C(Z,\nu)$ is a function of Z and the momentum, where ν is the inverse length in angstroms, $Å^{-1}$.

The general effect of $C^2(Z,\nu)/Z^2$ is to decrease the Thomson cross section more extremely for backward scattering, for high E, and for low Z. This effect is opposite to the effect of $I(Z,\nu)/Z$ on $K(\alpha,\nu)$ in incoherent

(Compton) scattering. For a given Z, $C(Z,\nu)$ decreases from $C(Z,0) = Z$ to $C(Z,\infty) = 0$.

$C(Z,\nu)$ is a rapidly decreasing function of μ as μ varies from + 1 to −1, and therefore the coherent cross section is peaked in the forward direction. At high energies of the incoming photon, coherent scattering is strongly forward, and thus, coherent scattering can usually be ignored.

The parameter ν is the inverse length of the recoiling electron,

$$\nu = \sin(\theta/2)/\lambda = \kappa\alpha\sqrt{1-\mu} \quad , \tag{5}$$

where

$$\kappa = \frac{mc^2}{hc\sqrt{2}} = 29.1445 \text{ Å}^{-1} \quad . \tag{6}$$

The maximum value of ν is

$$\nu_{\max} = \kappa\alpha\sqrt{2} = 41.2166\alpha \tag{7}$$

at $\mu = -1$. The square of the maximum value is

$$\nu^2_{\max} = 1698.8038\alpha^2 \quad . \tag{8}$$

The qualitative features of $C(Z,\mu)$ are shown in Fig. 3.

In MCPLIB04 the coherent form factor $C(Z,\nu)$ is truncated at momentum transfer $\nu = 6$ Å^{-1}. Thus, the energy (in MeV) above which the truncation takes place is

$$E > \frac{\nu}{29.1445 \times 1.956917 \times \sqrt{1-\mu}} = \frac{0.1052015}{\sqrt{1-\mu}} \quad . \tag{9}$$

Above this momentum, MCNP/X sets the form factor to 0. That is, there is no fully backward scatter, $\mu = -1$ for $E > 0.07438874$ MeV. There is no backscatter, $\mu < 0$ for $E > 0.1052015$ MeV.

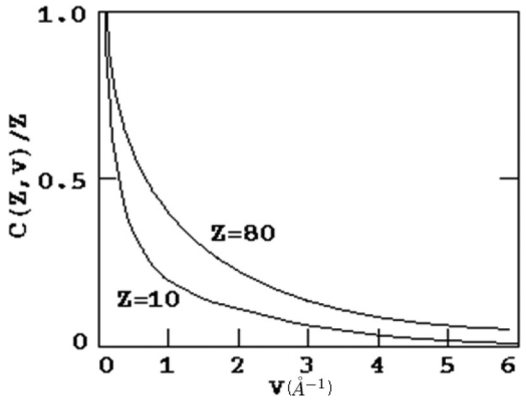

Fig. 3. Coherent photoatomic scattering form factors.

Figures 4 through 13 show the angular distributions of photons from coherent scatter for H, He, Fe, U, and Fm. The plots were generated statistically from MCNPX27C using $E = 0.1052015$ MeV incident photons (Figs. 4 through 8) and 1.7 MeV incident photons (Fig. 9 through 13). MCPLIB04 (blue dashed line) (color online) and MCPLIB05T (black solid line) results are overlaid. The MCPLIB04 results have no backscatter at these energies, whereas backscatter is apparent for MCPLIB05T for the heavier elements.

II. NEW PHOTOATOMIC LIBRARY

A new ACE-format photoatomic data library has been developed for MCNP/X. It has been tentatively named MCPLIB05 and is referred to herein as MCPLIB05T. These data, other than form factors, are identical to those in the predecessor photoatomic library, MCPLIB04. The only difference is the new form factor data in MCPLIB05T, which come directly from ENDF/B-VII (rev. 0).

The MCPLIB04 form factor data were provided in three blocks:

1. 21 incoherent form factors for both photon collision physics (COLLIDP) and next-event estimators (CALCPS)
2. 55 integrated coherent form factors for photon collision physics
3. 55 coherent form factors for next-event estimators.

Each of the form factor blocks had a corresponding hardwired momentum grid in a single-precision MCNP/X data statement:

1. 21 incoherent form factor momentums with a maximum value of 8 Å^{-1}
2. 55 integrated coherent form factor squared momentums. These were merely squares of the values in the following third block, the coherent form factor momentum grid with a maximum value of 36 Å^{-2}.
3. 55 integrated coherent form factors momentums with a maximum value of 6 Å^{-1}.

These grid values remained unchanged for 35 years since the predecessor code, MCP, in 1973.

The form factors in MCPLIB05T from ENDF/B-VII (rev. 0) are on incoherent and coherent momentum grids of arbitrary length. Consequently, the incoherent and coherent momentum grids are provided in the MCPLIB05T files for each element rather than hardwired for all elements in MCNP/X data statements. Thus, the MCPLIB05T form factor data consist of five blocks: incoherent momentum grid, incoherent form factors, coherent momentum grid, integrated coherent form factors, and coherent form factors.

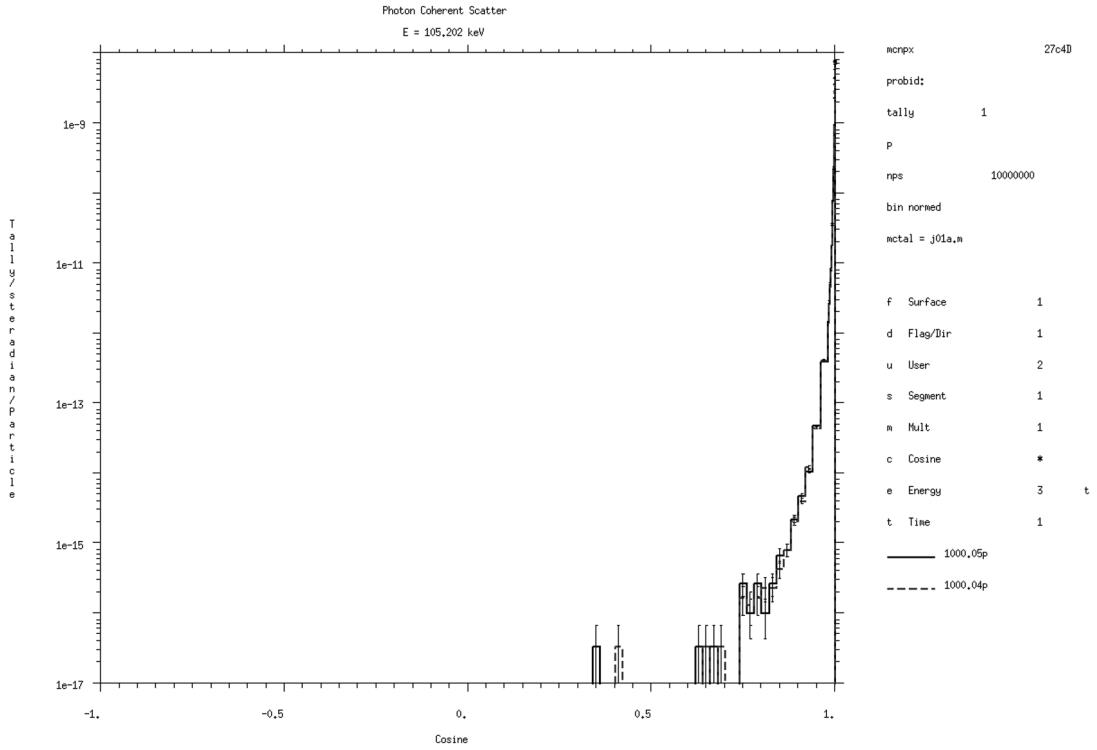

Fig. 4. Angular distribution of coherent (Thomson + form factors) scattering of 0.1052015-MeV photons on hydrogen. MCPLIB04 data are the dashed blue line (color online), and data from MCPLIB05T are the black solid line extending from $-1 < \mu < 1$.

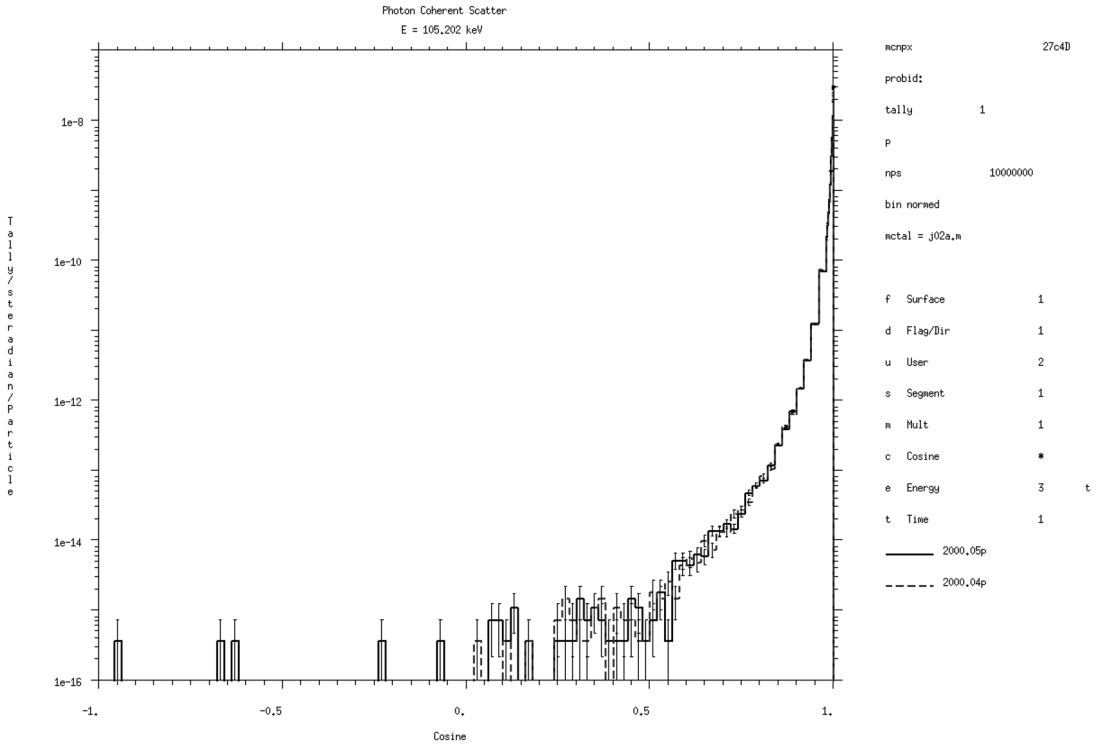

Fig. 5. Angular distribution of coherent (Thomson + form factors) scattering of 0.1052015-MeV photons on helium. MCPLIB04 data are the dashed blue line (color online), and data from MCPLIB05T are the black solid line extending from $-1 < \mu < 1$.

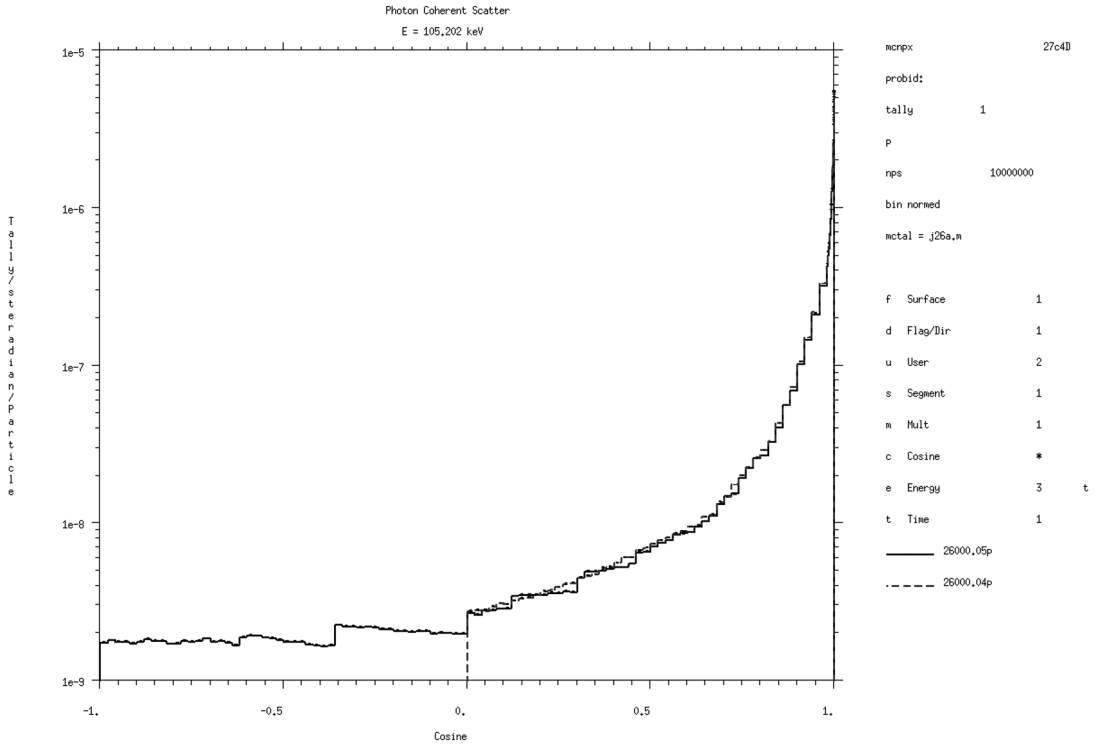

Fig. 6. Angular distribution of coherent (Thomson + form factors) scattering of 0.1052015-MeV photons on iron. MCPLIB04 data are the dashed blue line (color online), and data from MCPLIB05T are the black solid line extending from $-1 < \mu < 1$.

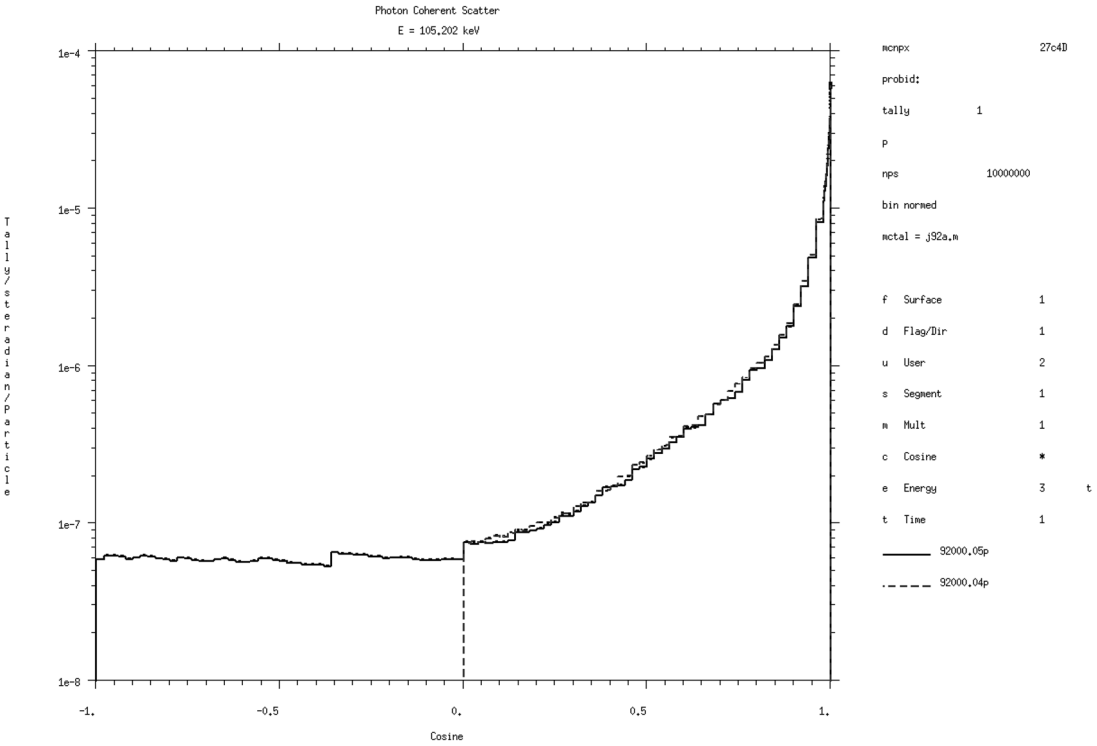

Fig. 7. Angular distribution of coherent (Thomson + form factors) scattering of 0.1052015-MeV photons on uranium. MCPLIB04 data are the dashed blue line (color online), and data from MCPLIB05T are the black solid line extending from $-1 < \mu < 1$.

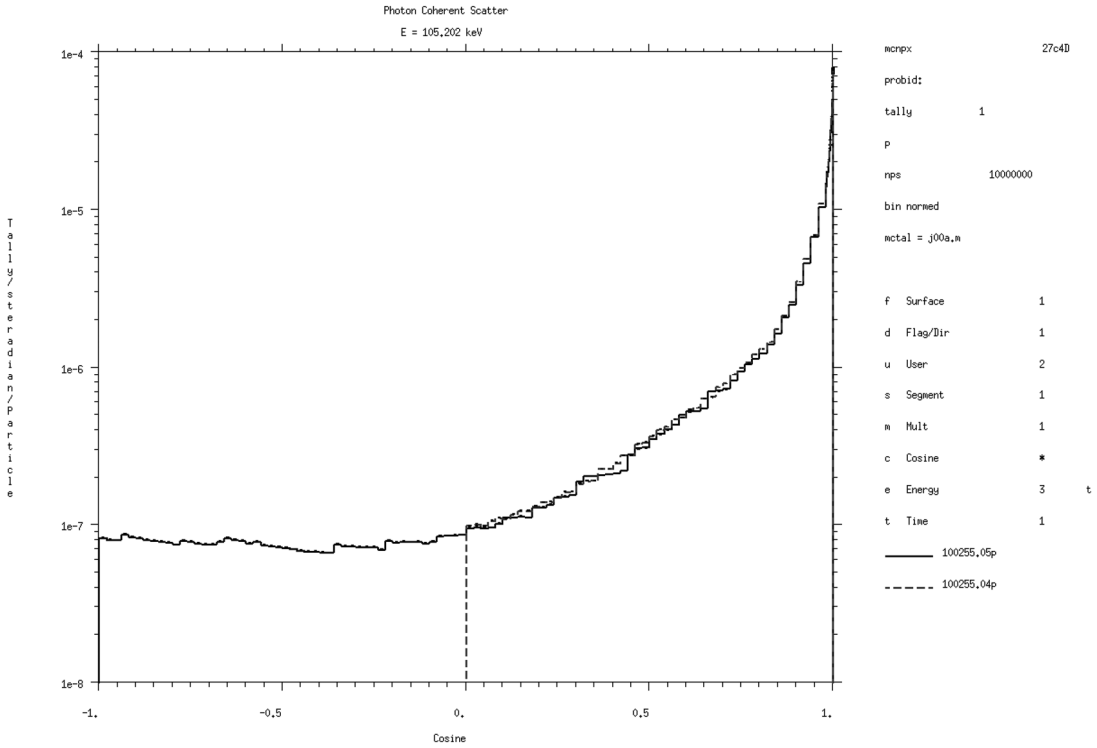

Fig. 8. Angular distribution of coherent (Thomson + form factors) scattering of 0.1052015-MeV photons on fermium ($Z = 100$). MCPLIB04 data are the dashed blue line (color online), and data from MCPLIB05T are the black solid line extending from $-1 < \mu < 1$.

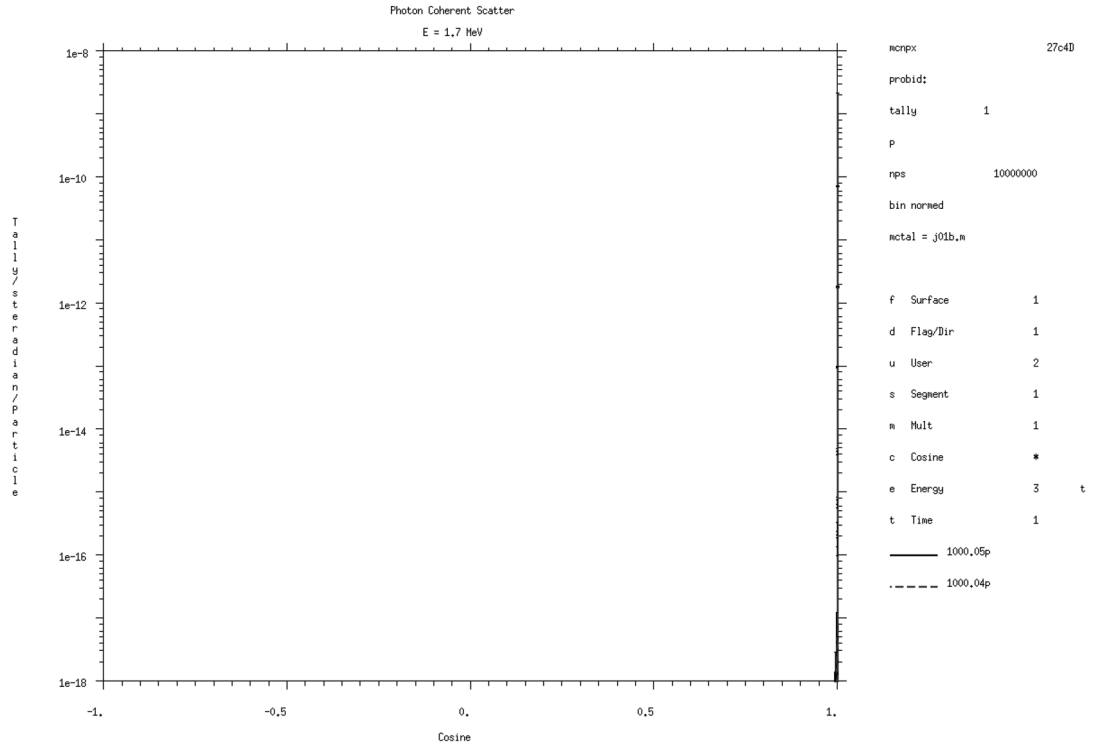

Fig. 9. Angular distribution of coherent (Thomson + form factors) scattering of 1.7-MeV photons on hydrogen. MCPLIB04 data are the dashed blue line (color online), and data from MCPLIB05T are the black solid line extending from $-1 < \mu < 1$. Both functions are nearly δ-functions at $\mu = 1$ and are therefore hard to see at the extreme right of the figure.

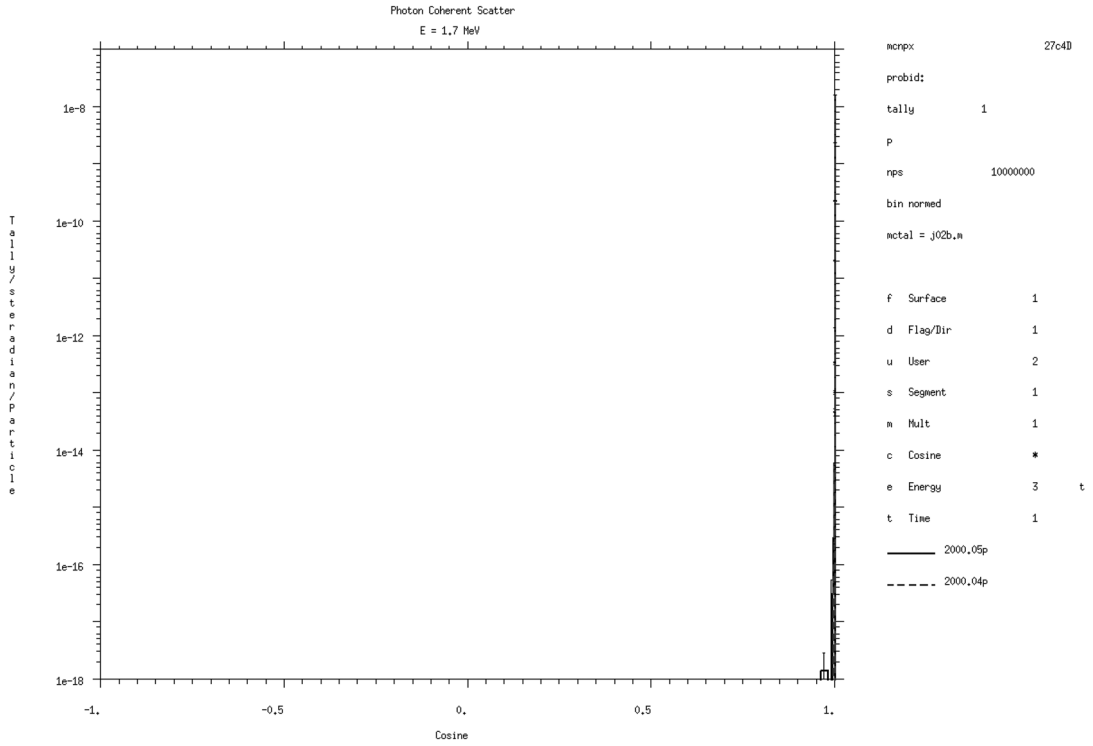

Fig. 10. Angular distribution of coherent (Thomson + form factors) scattering of 1.7-MeV photons on helium. MCPLIB04 data are the dashed blue line (color online), and data from MCPLIB05T are the black solid line extending from $-1 < \mu < 1$. Both functions are almost δ-functions at $\mu = 1$ and are therefore hard to see at the extreme right of the figure.

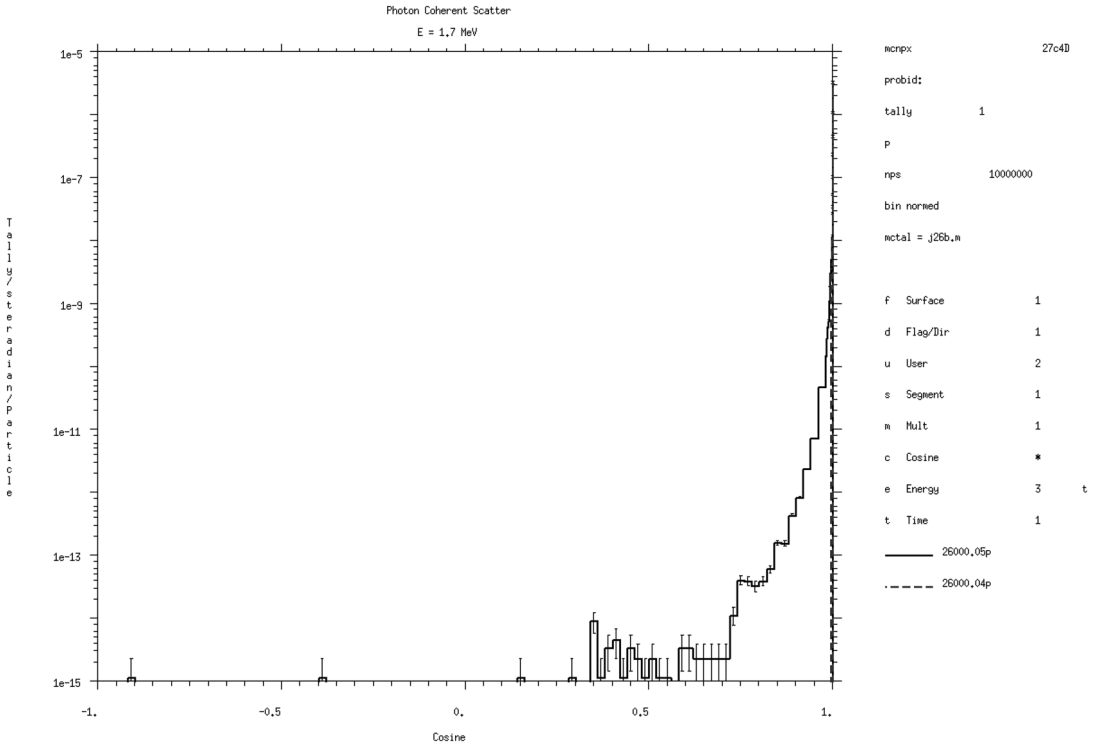

Fig. 11. Angular distribution of coherent (Thomson + form factors) scattering of 1.7-MeV photons on iron. MCPLIB04 data are the dashed blue line (color online), and data from MCPLIB05T are the black solid line extending from $-1 < \mu < 1$. The MCPLIB04 values are nearly a δ-function at $\mu = 1$ and are therefore hard to see at the extreme right of the figure.

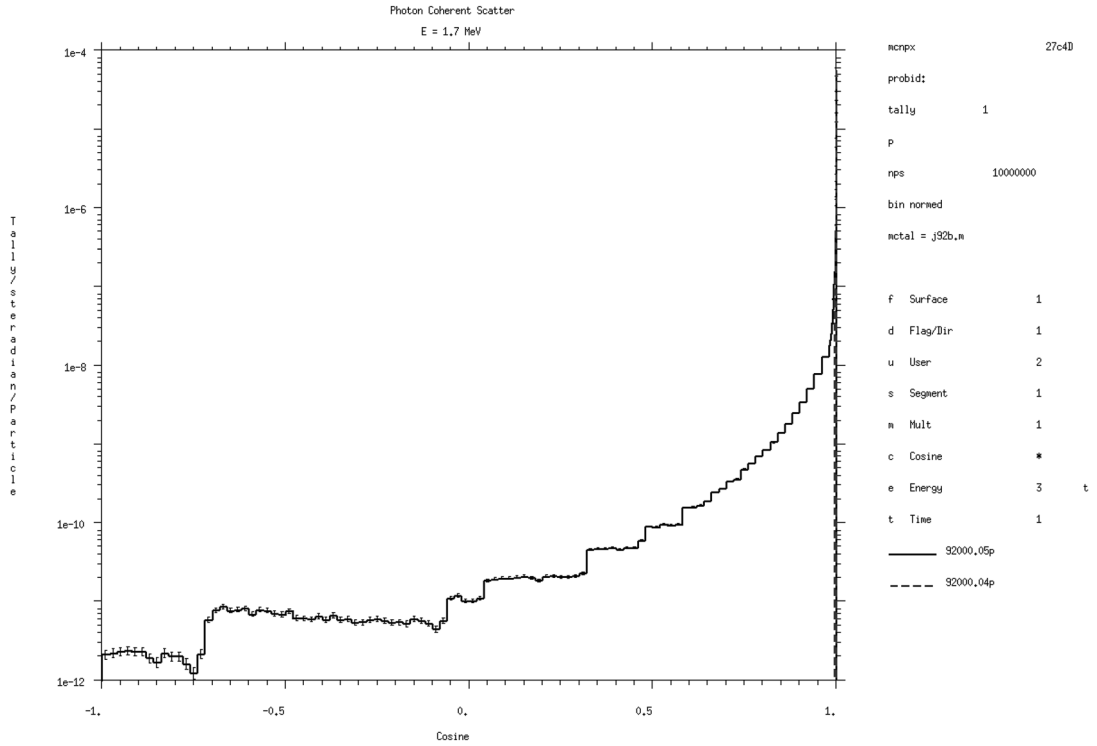

Fig. 12. Angular distribution of coherent (Thomson + form factors) scattering of 1.7-MeV photons on uranium. MCPLIB04 data are the dashed blue line (color online), and data from MCPLIB05T are the black solid line extending from $-1 < \mu < 1$. The MCPLIB04 values are nearly a δ-function at $\mu = 1$ and are therefore hard to see at the extreme right of the figure.

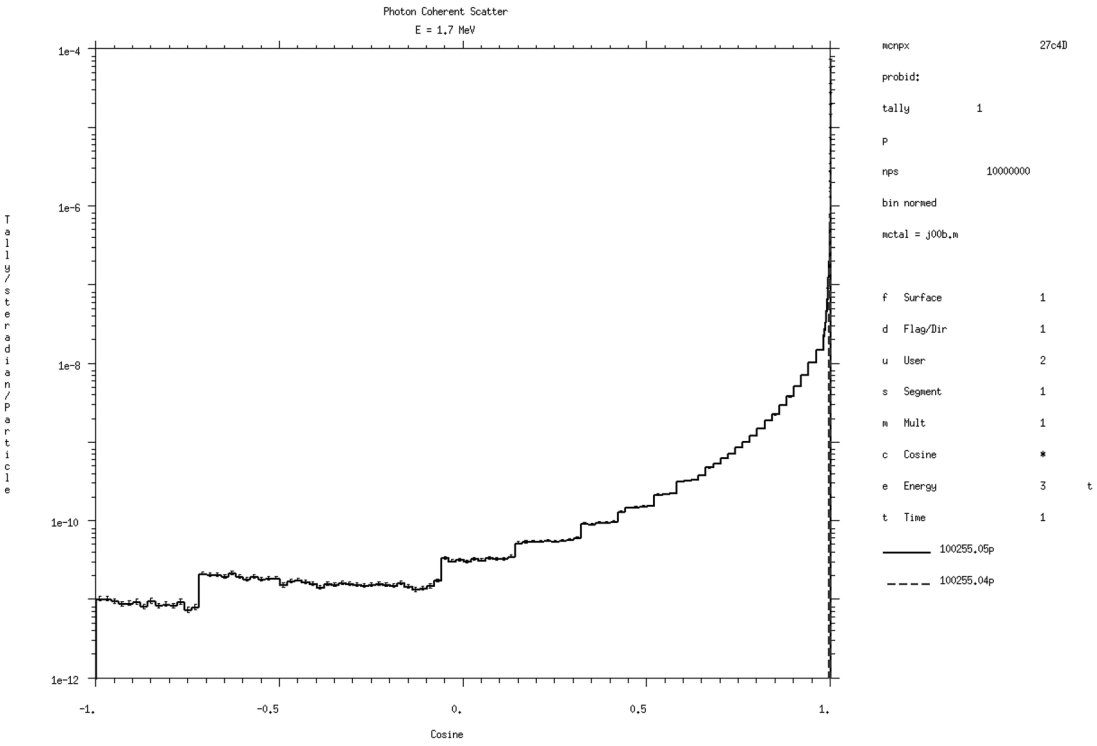

Fig. 13. Angular distribution of coherent (Thomson + form factors) scattering of 1.7-MeV photons on fermium. MCPLIB04 data are the dashed blue line (color online), and data from MCPLIB05T are the black solid line extending from $-1 < \mu < 1$. The MCPLIB04 values are nearly a δ-function at $\mu = 1$ and are therefore hard to see at the extreme right of the figure.

TABLE III

Energy and Momentum Limits for MCPLIB04 and MCPLIB05T

	Maximum Form Factor Values	
	MCPLIB04	MCPLIB05T
Incoherent momentum ($Å^{-1}$)	8	10^9
Coherent momentum ($Å^{-1}$)	6	10^9
Incoherent FF[a] energy (MeV) $\mu = 0$	0.1402687	1.753360×10^7
Incoherent FF energy (MeV) $\mu = -1$	0.09918494	1.239811×10^7
Coherent FF energy (MeV) $\mu = 0$	0.1052015	1.753360×10^7
Coherent FF energy (MeV) $\mu = -1$	0.07438874	1.239811×10^7
Photon transport energy (MeV)	10^5	10^5

[a]FF = ■■■.

The integrated coherent momentum grid is not stored because it is simply the square of the values of the coherent momentum grid.

The integrated coherent form factors do not come from ENDF/B-VII but were generated separately using an integration routine extracted from NJOY (Ref. 9). The integrated form factors are the cumulative values of the integral

$$\int [I(Z,\nu)]^2/\delta(\nu^2) \ , \qquad (10)$$

integrated on the integrated coherent momentum grid of ν^2 values.

The momentum and energy limits of the new photoatomic form factors in MCPLIB05T are given in Table III. Since the data are now of arbitrary length, future versions of MCPLIB can change these limits easily.

The NJOY nuclear data processing system is undergoing modification to enable future generation of photoatomic data libraries with modern form factor data in the new format.

III. MCNP/X MODIFICATIONS

A new version of MCNP/X has been developed to identify and use the new MCPLIB05T data and yet retain backward compatibility, including tracking, when MCPLIB04 is used.

The COLLIDP and CALCPS logic is unchanged, with the following exceptions:

1. The incoherent and incoherent momentum grids are now read from the cross-section data blocks 1 and 3 rather than using hardwired data.

2. The coherent form factor squared momentums are calculated as needed from the coherent form factor momentum grid.

Using the squares of values in the coherent form factor momentum grid (block 3) rather than having these squares stored separately in a hardwired single-precision MCNP/X data statement occasionally results in slight tracking differences when MCPLIB04 data are used. Using the same logic for MCNPLIB04 and MCPLIB05T ensures that no error has been introduced in the collision physics or next-event estimators.

The principal upgrade to MCNP/X is that when the old format of form factors is input from MCPLIB04 (or preceding libraries), it is recognized because the incoherent form factor block is always 21 entries long; the new format MCPLIB incoherent form factors (MCPLIB04) consist of two blocks (momentum grid and form factors) and are thus always an even number length and never 21 entries long. Old coherent format form factor blocks 1, 2, and 3 are moved to form factor blocks 2, 4, and 5. Then, the momentum grids (missing in MCPLIB04) are provided by a data statement and put in blocks 1 and 3. These MCNP/X changes are summarized in Table IV. Although the upgraded MCNP/X works with both MCPLIB04 and MCPLIB05T, older MCNP/X versions only work with MCPLIB04 and crash during initiation if MCPLIB05T is called.

Photoatomic data in the new format are input without any changes since they are already in the format the collision physics and next-event estimators expect.

There are no user interface changes. Whether MCPLIB05T or a preceding library is used is determined by the usual specifications on the MCNP/X materials cards.

Note that MCNP/X generally assumes that input cross sections and secondary distributions will be processed with linear-linear interpolation. (A notable exception is the photoatomic cross section data excluding the form factors.) The new MCNP/X (nearly) tracks the old MCNP/X when old MCPLIB04 data are used because the interpolation of form factor data continues to be linear-linear. But the form factors in ENDF/B-VII require log-log interpolation. The solution for neutron transport is to have NJOY "linearize" the data—that is, insert enough extra data points so that linear-linear interpolation matches log-log interpolation to a specified tolerance (generally an error <0.005.) Because the form factors in MCNP/X use linear-linear interpolation and the data in the new library are not linearized, the form factors result in "stair step"–type angular distributions as seen in Figs. 6, 12, and 13. Each step is approximately a factor of 2 high. Thus, the histogram shape of the coherent scatter rather than a smooth logarithmic shape is due to the interpolation. Correcting this interpolation is complicated by being unable to recognize the interpolation scheme in the ACE-format data; it will be addressed in later MCNP/X

TABLE IV

Comparison of New and Old MCNP/X and MCPLIB

	MCPLIB04	Old MCNP/X	MCPLIB05T	New MCNP/X
Incoherent FF momentum grid		Data statement 21-point grid	Variable grid from ENDF/B-VII	
Incoherent FF	21 values—force fit by NJOY		Values from ENDF/B-VII	
Coherent FF grid		Data statement 55-point grid	Variable grid from ENDF/B-VII	
Coherent FF grid squared		Data statement 55-point grid		Unneeded
Integrated coherent FF	55 NJOY integrated values		External code integration of coherent form factor	
Coherent FF	55 values—force fit by NJOY		Values from ENDF/B-VII	

versions. Its effect is smaller than neglecting backscatter altogether as in MCPLIB04 but could be important when backscatter is finely tallied in a simulation.

IV. VALIDATION AND VERIFICATION

The new MCPLIB05T photoatomic library and modified MCNP/X have been validated and verified in a number of ways.

IV.A. MCNP/X Tests

The MCNPX27B ~450-problem test set was used with the modified MCNP/X and the old MCPLIB04 library. All but five of the problems track identically. The five exceptions were traced to the round-off of coherent form factor squared momentums that now use ν^2 from ν rather than from a hardwired single-precision table of ν^2 values.

The fact that the new MCNP/X uses the same pieces of code for both MCPLIB04 and MCPLIB05T collision physics and next-event estimators ensures that use of the new form factors is robust.

Point detectors and surface tallies of the coherent scatter were compared and had excellent agreement.

The modified MCNP/X was further modified (MCNPXx) to allow individual photon reactions (incoherent, coherent, photoelectric, and pair production) with and without form factors to be run. These results were plotted for a number of nuclides and compared. The coherent scatter angular distributions in Figs. 4 through 13 are from MCNPXx.

MCNPX tally tagging was also used to plot individual reactions in the new MCNP/X code. This test is almost as good as the one above except that tagging cannot be used in conjunction with point detectors or the FTn INC option, which was used to segregate single-collision events.

IV.B. MCPLIB05T Tests

To check the methodology used to make MCPLIB05T, the same method was used to insert old form factors into the new library to make MCPLIB04x. MCPLIB04 and MCPLIB04x were identical, proving that insertion of the new form factors did not corrupt other photoatomic data.

Plots of MCPLIB04 and MCPLIB05T individual photon reactions were made and compared, particularly plots of coherent scatter. As expected, the only differences were for incoherent and coherent scattering, and these were as expected.

Direct comparison of MCPLIB04 and MCPLIB05T form factors was made and tabulated. For incoherent form factors with $\nu < 8$, the biggest difference was 6.55×10^{-6}% for $Z = 10$. For coherent form factors with $\nu < 6$, the largest difference was 0.00400 for $Z = 76$, and only four other elements had differences >0.003. In percentage terms, the differences were between 2 and 3% for $35 < Z < 39$ and more than 3% for $Z < 10$. The large percent differences were all for small ν where the form factor values were small. For the coherent integrated form factors, the largest absolute error was 0.00324 for $Z = 93$, and the largest percent error was 0.605% for $Z = 55$. These differences are mostly attributable to the linear-linear interpolation on the steeply rising forward scattering (low ν) coherent form factors. Thus, the new and old form factors have excellent agreement, as would be expected, below the ν truncation value.

V. RECOMMENDATIONS

A new ACE-format photoatomic library of 100 elements, tentatively named MCPLIB05T, has been developed to use the latest ENDF/B-VII photoatomic incoherent and coherent form factors. MCNP/X has been upgraded to recognize and read this library yet maintain backward compatibility when using the old MCPLIB04 library. MCPLIB05T should become the default photoatomic library for MCNP/X, and the modifications made to use it should become standard in MCNPX and MCNP6.

As funding permits in the future, MCNP/X should be upgraded to use log-log interpolation of form factors. But first, a number of issues would need to be resolved. Should backward compatibility be maintained by still using linear-linear interpolation when MCPLIB04 is detected? Should both coherent and integrated coherent form factors use log-log interpolation even though linear-linear interpolation presently appears fully adequate for incoherent form factors?

Another MCNP/X improvement would be to use binary searches to look up form factor data. When the form factors were limited to 21- and 55-point grids, binary lookup was not needed. Now the new algorithm is a few percent slower due to the linear lookup, although in realistic transport problems the coherent scatter time should be insignificant compared to all the other aspects of transport.

NJOY should be upgraded to correctly process future photoatomic data libraries. Presently, it cannot process any, and that is why the approach reported herein—namely, inserting ENDF/B-VII form factors directly into MCNPLIB04—was used. NJOY should also thin data to eliminate wasteful duplicate form factors at successive grid points in the asymptotic regions of the form factor data. Finally, if log-log interpolation is not used for form factors in MCNP/X, then NJOY should linearize the form factor data so that linear-linear interpolation gives better agreement.

Finally, a number of additional improvements could be made to MCNP/X photon physics in the long term:

1. Extend the range of photoatomic interactions below 1 keV.

2. Investigate Delbrück scattering and nuclear Thomson scattering and incorporate them as merited.

3. Anomalous scattering factors are provided in the ENDF/B-VI photoatomic data and perhaps should be included in the MCNP/X physics.

4. Polarization should be studied and perhaps included in MCNP/X for incoherent Doppler broadening.

5. Improved photonuclear physics is needed, particularly the inclusion of more isotopes, separation of photofission from other inelastic reaction channels, and addition of NRF lines.

ACKNOWLEDGMENTS

This work was performed by TechSource, Inc., under a contract with Brookhaven National Laboratory, and in collaboration with the University of California Berkeley, Lawrence Berkeley National Laboratory, and Los Alamos National Laboratory.

REFERENCES

1. D. B. PELOWITZ, "MCNPX User's Manual Version 2.6.0," LA-CP-07-1473, Los Alamos National Laboratory (2008); see http://mcnpx.lanl.gov.

2. X-5 MONTE CARLO TEAM, "MCNP—A General Monte Carlo N-Particle Transport Code, Version 5, Volume I, MCNP Overview and Theory," LA-UR-03-1987, Los Alamos National Laboratory (Apr. 24, 2003; revised Oct. 3, 2005); see http://mcnp-green.lanl.gov.

3. B. J. QUITER, B. A. LUDEWIGT, and V. V. MOZIN, "Nondestructive Spent Fuel Assay Using Nuclear Resonance Fluorescence," *Proc. Institute of Nuclear Material Management*, Tucson, Arizona, July 12–16, 2009 (2009).

4. C. J. LODWICK and H. B. SPITZ, "Modification to the Monte Carlo N-Particle Code for Simulating Direct, In Vivo Measurement of Stable Lead in Bone," *Health Phys.*, **94**, *6*, 519 (2008).

5. E. D. CASHWELL et al., "Monte Carlo Photon Codes: MCG and MCP," LA-5157-MS, Los Alamos National Laboratory (Mar. 1973).

6. D. E. CULLEN, J. H. HUBBELL, and L. KISSEL, "EPDL97: The Evaluated Photon Data Library, '97 Version," UCRL-50400, Vol. 6, Rev. 5, Lawrence Livermore National Laboratory (1997).

7. National Nuclear Data Center Web site: http://www.nndc.bnl.gov (current as of February 9, 2010).

8. M. C. WHITE, "Photoatomic Data Library MCPLIB04: A New Photoatomic Library Based on Data from ENDF/B-VI Release 8," LANL internal memorandum X-5:MCW-02-111 and LA-UR-03-1019, Los Alamos National Laboratory (2002).

9. R. E. MacFARLANE, "NJOY 99 Nuclear Data Processing System"; available at http://t2.lanl.gov/codes/njoy99/.